

https://doi.org/10.1070/QEL18070

Application of all-optical magnetometry for detection of weak magnetic fields generated by a current-carrying metallised track

E. Taskova, E. Alipieva, N. Stankova, V. Ranev, C. Andreeva, D.V. Brazhnikov

Abstract. **A pump–probe configuration is used to register zero-field level-crossing resonances in Rb vapour contained in a cell with antirelaxation coated walls. The scheme is applied to detect the weak magnetic field generated by a current-carrying micro-wire (metallised track). Such micro-wires can be employed in neural prostheses and hybrid bionic systems as micro-electrode arrays. More specifically, the operation of such live micro-wire belonging to a neuronal–electrode interface is demonstrated, which indicates the possibility of remote testing of the operation (conducting/non-conducting) of micro-wires for in neural implants.**

Keywords: *level-crossing resonances, electromagnetically induced absorption, atomic magnetometry, quantum sensors, microelectrode arrays, PDMS.*

1. Introduction

The rapid development of quantum magnetometry methods in recent years has been related to some of the most important tasks both in the field of applied and fundamental physics, which require the use of highly sensitive magnetometers. Among the possible applications are the medical ones, which include the use of optical pumped atomic magnetometers for diagnostics of cardiac diseases, brain studies, etc. [1–4]. Some of the recently demonstrated realisations surpass the standard technologies used in medicine, like for example the SQUID-magnetometers, both in terms of sensitivity reached and in the absence of cryogenic temperatures and power supply needs. Besides medicine, such magnetic field sensors find applications in geophysics [5], gravimetry [6], remote tomography of magnetic fields [7], etc.

This type of sensors operates on the basis of control of the atomic quantum state that is determined by the ambient magnetic field vector. One of the most interesting and promising nonlinear interference effects with application to magnetometry is the effect of coherent population trapping (CPT) and the related electromagnetically induced transparency (EIT) of the atomic medium. The effect consists in the preparation of an atomic medium (alkali atom vapour) in a coherent state, in which it does not absorb light resonant with the optical atomic transition. The effect is usually manifested as a narrow resonance in the medium transmittance (or fluorescence) in the dependence of the detuning between the frequency difference of the optical waves and the frequency difference of the atomic ground states involved (determined by the value of the magnetic field). In 1998 Akulshin et al. [8] showed experimentally the opposite effect, namely electromagnetically induced absorption (EIA), which is related to spontaneous transfer of anisotropy from the excited state to the ground atomic state [9].

The most relevant characteristics of this type of resonances is that their linewidth is determined only by the width of the ground-state atomic levels thus it is much lower than the natural linewidth of the optical transition (the so-called subnatural-width resonances). Different approaches are used to increase this lifetime, including an addition of noble or other molecular gases as a buffer gas in the cell, or depositing an antirelaxation coating on the cell walls. These measures lead to a significant decrease in the resonance contrast, and therefore different approaches have been proposed in order to comply with the contradicting requirements for obtaining high contrast and narrow linewidth using the standard realisation schemes.

A very convenient approach to study these effects is a so-called level-crossing magneto-optical (ground-state Hanle-type) configuration. It uses only one excitation wavelength, and the absorption/fluorescence signal is registered by scanning a magnetic field applied parallel or orthogonal to the light wave vector [10] and the resonance is centred at the position of the zero value of the magnetic field (see, for example, [11]).

A novel scheme was proposed for the preparation and registration of a coherent state on an open dipole transition, where the use of a buffer gas does not lead to suppression of the EIA signal in contrast to many other observation schemes. In this modified Hanle configuration, the EIA is due to the interaction of a probe beam with the atomic ground state, which is either aligned [12] or oriented [13] by a counter-propagating pump beam. The experimental results show that in this configuration the open transition can lead to an EIA signal with a linewidth of below kHz, with contrast approaching 100% (for comparison, the standard Hanle scheme for open transitions yields at best a contrast of around 10%).

E. Taskova, E. Alipieva, N. Stankova, V. Ranev Institute of Electronics, Bulgarian Academy of Sciences, boul. Tzarigradsko shosse 72, Sofia, Bulgaria;
C. Andreeva Institute of Electronics, Bulgarian Academy of Sciences, boul. Tzarigradsko shosse 72, Sofia, Bulgaria; Faculty of Physics, Sofia University, boul. J. Bourchier 5, Sofia, Bulgaria;
e-mail: c.andreeva@ie.bas.bg;
D.V. Brazhnikov Institute of Laser Physics, Siberian Branch, Russian Academy of Sciences, prosp. Lavrent'evs 15B, 630090 Novosibirsk, Russia; Novosibirsk State University, u. Pirogova 1, 630090 Novosibirsk, Russia;
e-mail: brazhnikov@laser.nsc.ru

Received 14 March 2022; revision received 29 April 2022
Kvantovaya Elektronika **52** (6) 544–548 (2022)
Submitted in English

A similar configuration has been used in [14], where a counter-propagating pump–probe scheme is applied for the D_1 line in K contained in a coated cell. It should be noted that in K the D_1 transitions cannot be considered 'open' due to the fact that the hyperfine splitting of the ground states (with $F_g = 1$ and 2) is smaller than the Doppler linewidth of the transition. It has been shown that for parallel linear polarisations of the pump and probe beams the registered resonances have a contrast reaching 70%. Similar values above 90% for the contrast were recently obtained in a configuration involving a (σ^+, σ^-) pump–probe polarisation, for excitation of the D_1 line in Cs contained in a buffer gas cell [13].

Recent experimental results were also obtained using two counter-propagating pump and probe beams with linear and mutually orthogonal polarisations, exciting the D_1 transition in Rb contained in a coated optical cell [15]. Taskova et al. [15] demonstrated that like for the standard Hanle configuration [16], the resonance obtained when scanning longitudinal magnetic field has a complex (double-Lorentzian) lineshape. It should be noted that the application of an additional small dc magnetic field orthogonal to the laser wave vector leads to a broadening of the resonance [13].

In the present work, we apply the configuration as described in [15] to detect the weak magnetic field generated by a current-carrying micro-wire (metallised track) for application in neural prostheses and hybrid bionic systems as micro-electrode arrays, namely detecting the operation of such neuronal–electrode interfaces [17]. The purpose is to evidence possibility of remote testing of the operation (conducting/nonconducting) of micro-wires in neural implants.

2. Experimental setup

The setup used is similar to that described in [15], and it is shown schematically in Fig. 1. In order to measure the cell transmission in a pump–probe configuration, a single laser beam is used, generating at 795 nm in resonance with the D_1 line of Rb, and its linear polarisation is controlled by means of a $\lambda/2$ plate. The beam, with a diameter of approximately 4 mm, is split into two orthogonally polarised beams by a polarising beam splitter (PBS). The pump beam $\boldsymbol{E}_{\text{pump}}$ (thick red line in Fig 1a; horizontal polarisation along the x axis in Fig.1b) has a power of 500 μW and it passes through the cell and aligns the ground-state level of the Rb atoms. The probe beam $\boldsymbol{E}_{\text{probe}}$ (thin green line in Fig. 1a) has orthogonal polarisation (vertical, perpendicular to the plane of Fig. 1a and directed along the y axis in Fig.1b) and a power of 8 μW. It is directed in the opposite direction by a set of mirrors to probe the state prepared by the pump beam and is registered by a photodiode (PD). This scheme allows for a very precise overlapping of the pump and probe beams with excellent subsequent separation and separate control of the pump and beam powers using neutral-density filters (not shown in the figure).

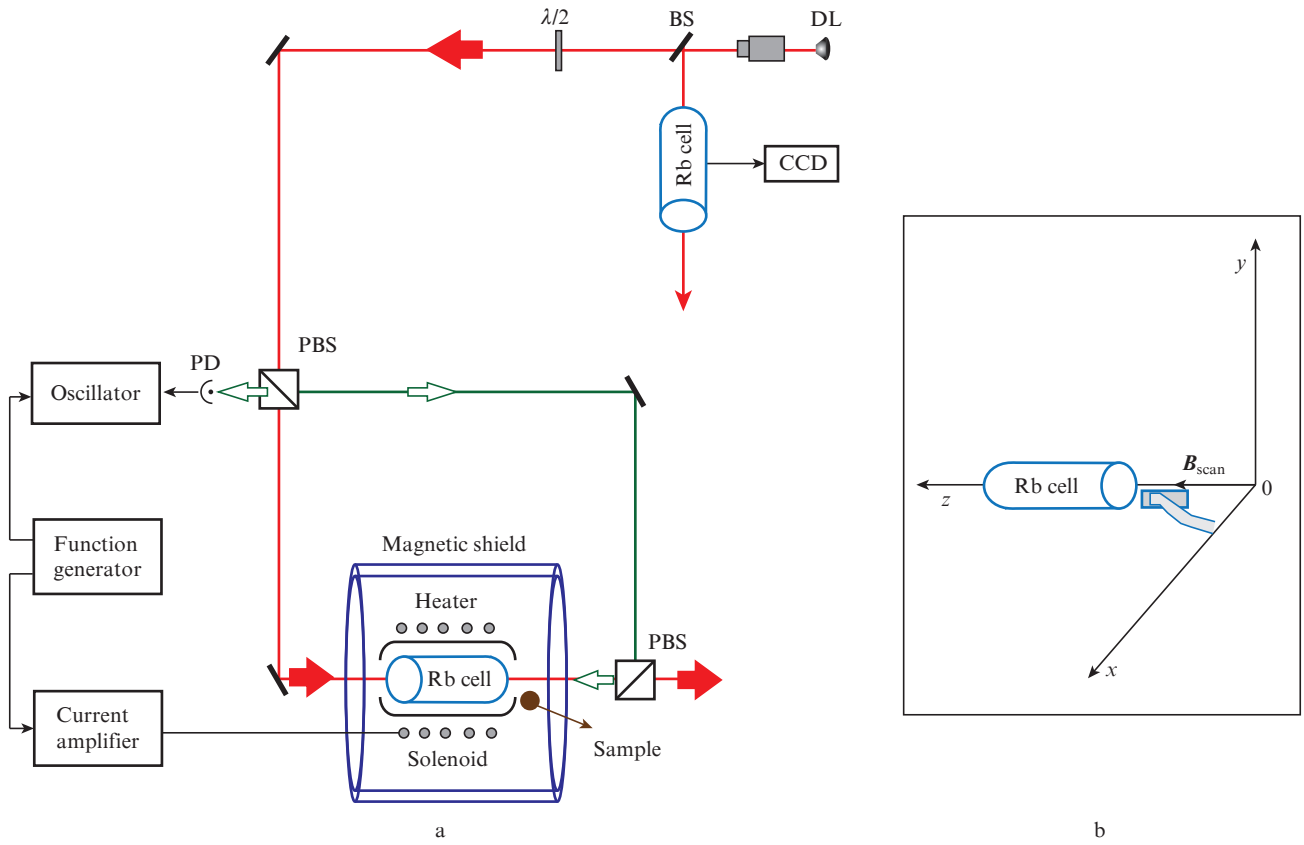

Figure 1. (Colour online) (a) Scheme of the experimental setup for registration of magneto-optical resonances in a Hanle configuration using pump and probe beams and (b) sample position with respect to the cell:
(DL) diode laser; (PBS) polarising beam splitter; (BS) beam splitter; (PD) photodiode. The pump and probe paths are shown by red and white arrows, respectively. The walls of the optical cell have an antirelaxation coating.

The Rb cell serving as a magnetic field sensor is a paraffin-coated ^{87}Rb cell, which is 2 cm in diameter and 2.5 cm long. Its temperature is kept around 40 °C. The cell is placed in a 30 cm long solenoid, providing a homogeneous dc magnetic field along the cell axis. Both the cell and the solenoid are placed in a two-layer magnetic shield that isolates the laboratory magnetic field. The laser frequency is controlled by monitoring the fluorescence from a second (reference) Rb vapour cell containing a natural mixture of Rb isotopes. The sample we test is placed in front of the cell, at a distance of around 10 mm from the 'front' window. As can be seen, for this position of the sample, the magnetic field generated is along the x axis. It is not homogeneous, but is decreasing along the cell.

When the magnetic field to be measured is longitudinal, it leads to a shift in the centre of the resonance with respect to the zero value of the scanned magnetic field. The value of the unknown magnetic field is directly estimated from the value of this shift (where the scanned magnetic field compensates the additional one).

As mentioned above, when the magnetic field to be measured is orthogonal, it leads to a broadening of the resonance and ultimately to its destruction. Thus, careful calibration of the signal width vs. the orthogonal magnetic field is needed. This has been realised by introducing a pair of Helmholtz coils with the known constant magnetic field/current, and registering the signal linewidth for different values of the orthogonal magnetic field provided by the coils.

3. Sample description

The technology for the sample preparation is based on surface modification and activation of optically transparent biocompatible polymers by pulsed laser irradiation for the development of neuronal–electrode interface technologies. These technologies are used to allow fine movements of the limbs, or partially restore vision, hearing, sense of pressure and touch, as well as control the functions of various organs such as heart, liver, central and peripheral nervous system, and muscles. This frontier, which combines biology and electronics into one, is known as bionics.

These neural implants can be realised by developing new materials and technologies for making micro-electrode arrays (MEAs) on biocompatible media such as neural–electrode interface devices for recording and/or stimulating nerve activity in a relevant part of the body. They are implanted in soft tissues like brain, spinal cord, muscles, and organs. A suitable material as a carrier of micro-electrode arrays is the synthetic polydimethylsiloxane (PDMS) elastomer, mainly due to its high biocompatibility and long-term biostability. In addition, it is non-toxic and has high gas permeability, elasticity and mechanical flexibility. The first two steps of fabrication of this type of a micro-electrode track is the following: (i) structuring and activation of the PDMS polymer surface by direct ns laser treatment (ablation) with a wavelength of 266 nm, pulse duration 15 ns, repetition rate 10 Hz; and (ii) functionalisation of the PDMS sample by autocatalytic (chemical) deposition of Platinum (Pt) on the activated areas – the so-called electroless metallisation. Figure 2 shows a photo of an array of such tracks before connecting the voltage supply wires (a) and a zoomed photo of one of the tracks with the connection seen at both ends (b). More details on the sample production process are presented in [18].

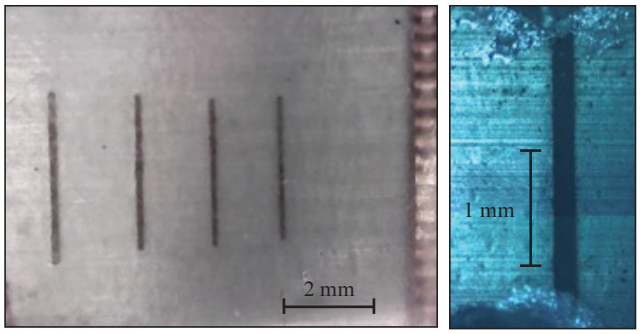

Figure 2. (Colour online) Photo of an array of metallised tracks (a) before and (b) after connecting the wires at the ends of one of the tracks.

The thickness of the sample is around 200 μm in view of the requirements for maximum flexibility in bending the implant device, and the track length is ca. 2 mm. For convenience, in the present measurements, the PDMS elastomer is placed on a glass substrate, which limits the distance between the micro-track and the cell window to about 10 mm.

4. Experimental results

Figure 3 presents the complex lineshape of the resonances obtained from the antirelaxation coated cell. As can be seen, it consists of a broader pedestal and a narrow resonance in the centre. Therefore, to analyse the obtained signal, we make a multiple-peak fit, with two Lorentzian profiles.

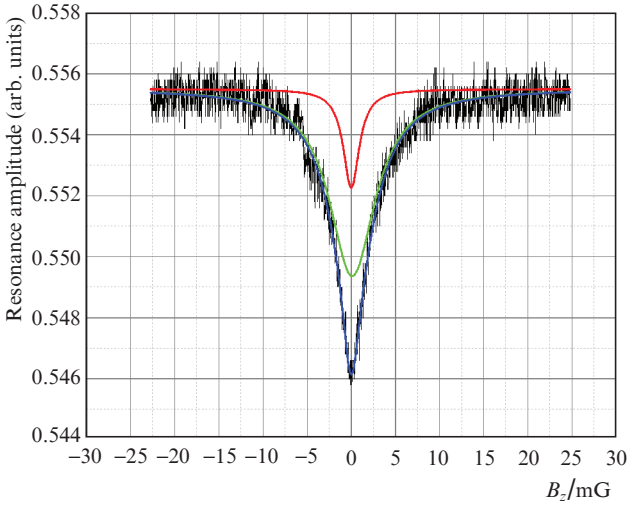

Figure 3. (Colour online) Resonance signal and its approximation by a double Lorentzian function (red and green curves).

Here we show the results from the fit of the control signal, that is, the signal without the sample with a compensated transverse magnetic field. The scanned longitudinal magnetic field of the solenoid is calibrated, and thus we have a linewidth of the narrow component of the signal of 2.2 mG.

Next, the signal linewidth should be calibrated with respect to the magnitude of the orthogonal magnetic field. Since the sample induces a magnetic field in the x direction

(see Fig. 1b), a Helmholtz coil (not shown in Fig. 1) with a known constant [mG mA^{-1}] was used to produce additional dc magnetic field around the sensor (i.e. the optical cell). For small transverse magnetic fields, the obtained calibration curve for the FWHM of the narrow component is shown in Fig. 4.

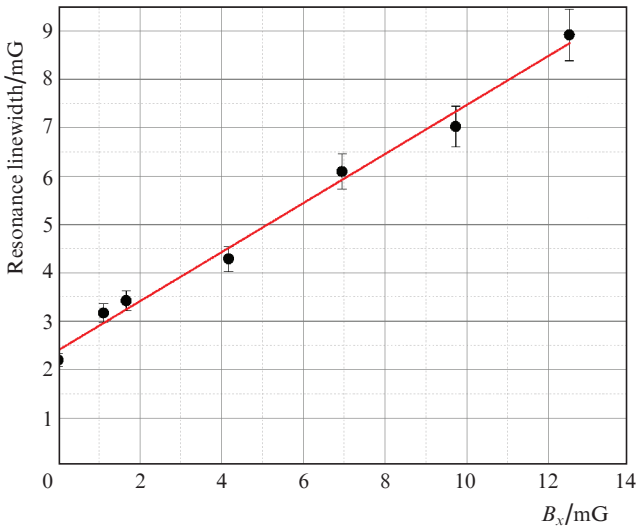

Figure 4. (Colour online) FWHM of the narrow component of the magneto-optical resonance as a function of the magnitude of a small transverse dc magnetic field B_x.

It can be seen that like in the case of [13], the dependence of the linewidth for the range of magnitudes of the B_x transverse magnetic fields used is linear, which is important for magnetometry.

After the calibration procedure, we place the sample in front of the cell, as shown in Fig. 1 and supply a voltage of 1 V. Normally, such micro-wires in bionic chips operate at slightly higher voltages [19], but with application of special cooling techniques. We do not cool our sample; therefore we did not apply a higher voltage. Initially, we also measured the current flow in the micro-track circuit; in this case, the reading was 15 mA, which yields a value for the resistivity of around 6 Ω $square^{-1}$. It should be noted that under normal testing conditions it would not be possible to add current measurement instrumentation into the operating sample circuit, and so the remote sensing should be reliable.

With the live micro-wire we register no shift of the resonance centre, but rather a broadening of the resonance signal, confirming that the magnetic field created by the sample in the chosen position is orthogonal to the scanning magnetic field. The obtained linewidth of the signal was ω = (4.3 ± 0.2) mG, corresponding to a transverse dc magnetic field B_x = (3.8 ± 0.4) mG. This uncertainty is estimated to about 5% from the fitting of the calibration line. This value is also confirmed from statistical analysis of repeated measurement results, yielding a relative error of 2%–5%.

It should be stressed that this signal is obtained at a relatively large distance of the sample from the sensor cell window (limited by the edge of the glass substrate holding the PDMS polymer), which confirms the feasibility of the method for remote contactless detection of live micro-wires.

5. Conclusions

We have shown that it is possible to detect the conductivity, and thus the operation, of current-carrying metallised tracks of micrometric thickness for use in neuro-bionic implants using a magneto-optical resonance of electromagnetically induced absorption in a pump–probe configuration. The micro-wire is prepared by nanosecond pulsed laser structuring and activation of PDMS with subsequent electroless Pt metallisation. The application of a 1 V supply to the micro-wire placed at a distance of 10 mm from the Rb vapour sensor allowed us to measure a transverse magnetic field of (3.8 ± 0.4) mG created by the sample, which is enough to discriminate between operating/nonoperating (conducting/nonconducting) condition.

Further work is in progress including replacing the magnetic shield-solenoid system by a system based on 3 mutually orthogonal pairs of Helmholtz coils in order to select different positions of the sample with respect to the Rb cell sensor and studying of the behaviour of the tracks in bending and twisting (without the glass substrate). More specifically, this includes measuring the magnetic signals induced by microelectrode arrays, by simulating their possible positions at *in vitro* and *in vivo* applications of the neural implants. Such technique could open new approaches for remote (non-invasive) detecting of the electrical reliability or defects of the neural-electrode interfacing devices when they are exposed to external stimuli including pressure, bending, twisting and stretching after their implantation in the body.

Acknowledgements. The work was supported by Russian Foundation for Basic Research (Grant No. 20-52-18004) and Bulgarian National Science Fund (KP-06-Russia/11) in the framework of a joint research project. D.V.B. also thanks the Russian Science Foundation (Grant No. 17-72-20089).

References

1. Bison G., Wynands R., Weis A. *Opt. Express*, **11**, 904 (2003).
2. Sander T.H., Preusser J., Mhaskar R., Kitching J., Trahms L., Knappe S. *Biomed. Opt. Express*, **3**, 981 (2012).
3. Belfi J., Bevilacqua G., Biancalana V., Cartaleva S., Dancheva Y., Moi L. *J. Opt. Soc. Am. B: Opt. Phys.*, **24** (9), 2357 (2007).
4. Marquetand J., Middelmann Th., Dax J., Baek S., Sometti D., Grimm A., Lerche H., Martin P., Kronlage C., Siegel M., Braun Ch., Broser Ph. *Clin. Neurophysiol.*, **132**, 2681 (2021).
5. Lipsich A., Barreiro S., Valente P., Lezama A. *Opt. Commun.*, **190**, 185 (2001).
6. Bongs K., Holynski M., Vovrosh J., Bouyer P., Condon G., Rasel E., Schubert C., Schleich W.P., Roura A. *Nat. Rev. Phys.*, **1**, 731 (2019).
7. Zhang R., Klinger E., Pedreros Bustos F., Akulshin A., Guo H., Wickenbrock A., Budker D. *Phys. Rev. Lett.*, **127**, 173605 (2021).
8. Akulshin A.M., Barreiro S., Lezama A. *Phys. Rev. A*, **57**, 2996 (1998).
9. Taichenachev A.V., Tumaikin A.M., Yudin V.I. *Phys. Rev. A*, **61**, 011802 (1999).
10. Dancheva Y., Alzetta G., Cartaleva S., Taslakov M., Andreeva C. *Opt. Commun.*, **178**, 103 (2000).
11. Alipieva E., Gateva S., Taskova E. *IEEE Trans. Instr. Meas.*, **54**, 2 (2005).
12. Brazhnikov D.V., Ignatovich S.M., Novokreshchenov A.S., Skvortsov M.N. *J. Phys. B: At. Mol. Opt.*, **52**, 215002 (2019).
13. Brazhnikov D.V., Vishnyakov V.I., Ignatovich S.M., Mesenzova I.S., Andreeva C., Goncharov A.N. *Appl. Phys. Lett.*, **119**, 024001 (2021).
14. Gozzini S., Lucchesini A., Marinelli C., Marmugi L., Gateva S., Tsvetkov S., Cartaleva S. *J. Phys. Conf. Ser.*, **700**, 012051 (2016).

15. Taskova E., Alipieva E., Andreeva C., Brazhnikov D. *J. Phys. Conf. Ser*., **1492**, 012011 (2020).
16. Alipieva E., Gateva S., Taskova E., Cartaleva S. *Opt. Lett*., **28**, 19 (2003).
17. Didier Ch.M., Kundu A., DeRoo D., Rajaraman S. *J. Micromech. Microeng*., **30** (10), 103001 (2020).
18. Stankova N., Nikolov A., Iordanova E., Yankov G., Nedyalkov N., Atanasov P., Tatchev D., Valova E., Kolev K., Armyanov S., Karashanova D., Fukata N. *Polymers*, **13**, 3004 (2021).
19. Gad P., Choe J., Nandra M.S., Zhong H., Roy R.R., Tai Yu-Chong, Edgerton V.R. *J. NeuroEng. Rehabil*., **10**, 2 (2013).